DEVELOPING STRATEGIES FOR PREDICTING LOCATIONS OF PAST HYDROTHERMAL ACTIVITY ON MARS. J. H. P. Oosthoek[1], A.P. Rossi[1], E. J. Carranza[2], and V. Unnithan[1], [1]Jacobs University Bremen, Germany, j.oosthoek@jacobs-university.de, [2]James Cook University, Townsville, Australia.

Introduction: It is increasingly recognized that hydrothermal activity has occurred on Mars [e.g. 1]. Geomorphological and mineralogical evidence show that Mars hosted at some point and for some time a hydrosphere [e.g. 2]. Massive volcanic provinces and giant rift systems occur which could have harbored hydrothermal systems [1]. Moreover Mars' surface is saturated with impact craters, varying from a few meters to thousands of kilometers in diameter [3]. Impacts therefore provided another heat source, possibly resulting in impact-induced hydrothermal activity (IIHA) and associated mineralization. 'Signals' of hydrothermal activity in impact craters could include the occurrence of crater mounds [4], crater deltas [5], possible crater lake deposits [6], CRISM derived clay signatures inside craters [7] and valley networks around crater rims [8].

The spatial pattern is investigated to determine if the signals are random, i.e. controlled locally by the impacts themselves, or non-random and controlled by the surrounding pre-impact structure and geology.

Methods: Spatial statistics methods, developed by Carranza et al. [9-10], were used to investigate the spatial pattern of these localities, on a global and regional scale. To enable analysis on a global scale the methodologies have been adapted from 2D map-projected to full geodesic analysis on a sphere.

The first step is *'spatial pattern analysis'* where the randomness (point pattern analysis), scale dependency (fractal analysis) and preferred orientations (fry analysis) of the spatial pattern are under investigation. The real points are compared with generated random points of complete spatial randomness (CSR).

The second step is *'spatial association analysis'* where the structural control by various geological 'features' (i.e. faulting, volcanism, multi-ring basins, mineralogy, gravity, magnetics, gamma ray spectrometry) will be quantified (distance distribution analysis), resulting in either a random (none), positive or negative spatial association. On the regional scale geological mapping and structural analysis will be performed to aid the deriving of a conceptual model possibly explaining the associations. The conceptual model together with the spatial association evidence (in the form of e.g. hyperspectral band-ratio maps and distance-to-'feature' maps) will be the input for knowledge-guided data-driven modeling leading to prediction maps of undiscovered locations of hydrothermal activity. Selected predicted localities will be further investigated with thorough geological (mineralogical/geomorphological) mapping.

The software used is 1) custom made python scripts for global 'geodesic' analysis using equal-spaced Geodesic Grids of various resolutions [11], 2) DotProc software for 2D Fry Analysis [12], 3) The R Project for Statistical Computing [13], 4) ESRI ArcGIS, the ArcGIS Spatial Data Modeler plugin [14] and various ArcGIS plugins by Jenness Enterprises [15] and 5) PlanetServer (Oosthoek et al., this volume #2523), for online access and analysis of remote sensing data.

Initial results: The workflow started by focusing on developing the methodology and collecting published input data.

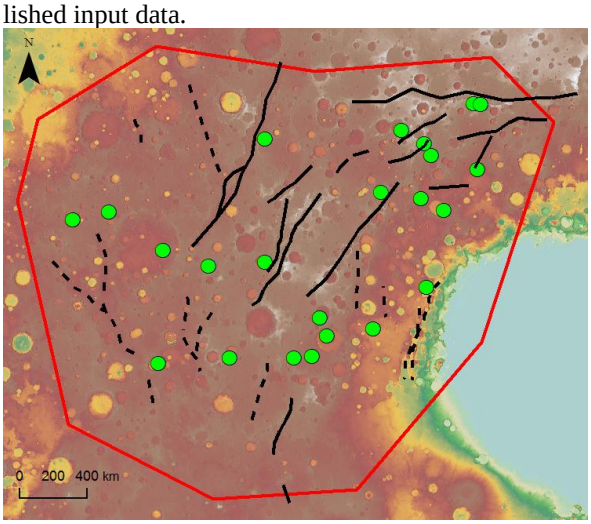

Figure 1. *Noachis Terra ROI (red border). Green are localities with CRISM-derived Fe/Mg Smectite clay signatures [7]. Solid black lines are mapped lineaments elaborating on work by Knapmeyer et al. [16]. Dashed lines need further investigation.*

A regional study focused on a distinct cluster in Noachis Terra consisting of 23 localities with CRISM-derived Fe/Mg Smectite clay signatures [7] (Fig. 1). Extensional fault lineaments, also shown in Fig. 1, were mapped in ArcGIS using MOLA gridded data. Knapmeyer et al. [16] lineaments were used as a basis.

The minimum and maximum (geodesic) distances between these locations are 44.1 km and 2616 km, respectively. Point Pattern Analysis following Carranza [9] encompassed the comparison with 23 CSR points. The mean values of 6 orders of neighborhood distances of both the real and CSR are shown in Table

1. The real means are all smaller than the CSR means which points to a clustered spatial pattern.

Order	Real mean (m)	CSR mean (m)
1	239874.2366	1121478.473
2	372820.2286	1468666.939
3	467512.2579	1884212.315
4	536078.9375	2156356.743
5	607942.6735	2451028.04
6	684988.6354	2632570.994

Table 1. *Neighborhood distances.*

The box counting method was used to perform fractal analysis. A log-log box counting plot of the 23 localities shows a kink in the slope around 300 km (Fig. 2). On Earth this is known to be caused by geological processes acting on different scales. The CSR points however also show the same kink. The usability of this approach therefore needs to be further investigated.

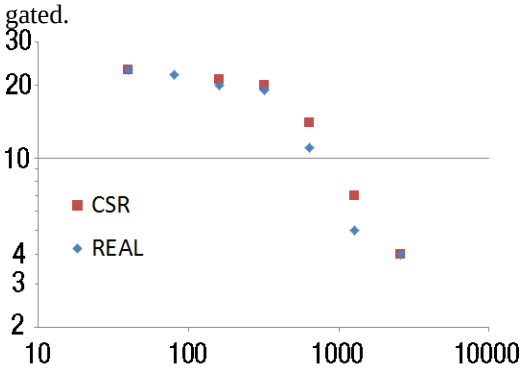

Figure 2. *Box counting plot (log-log).On the x-axis is the pixel size (km), on the y-axis the count of pixels with points.*

Fry Analysis was performed and the preferred orientations, together with preferred orientations of the mapped fault lineaments, are shown in Fig. 3. The two diagrams don't show a clear and distinct similarity in the orientations.

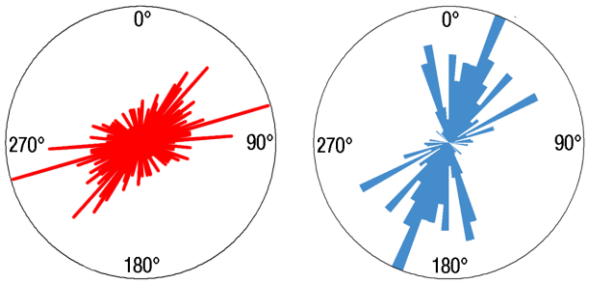

Figure 3. *Rose diagrams of preferred orientations through Fry Analysis (red) and faults preferred orientations (blue).*

As part of spatial association analysis a cumulative relative frequency distribution (CRFD) of the distances between the clay localities and the interpreted faults was calculated (Fig. 4). As a comparison also distances between the faults and CSR points were determined. The clay locality distributions plot predominantly below the CSR. This would suggest a negative spatial association and needs to be further investigated.

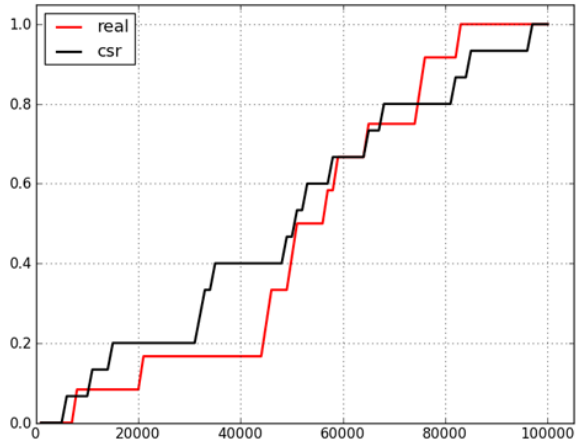

Figure 4. *Cumulative relative frequency distribution plot.*

Outlook: The methodology will be further fine-tuned so it can be easily applied to various location datasets. Possibly crater locations themselves will be used as CSR points. More thorough structural mapping of Noachis Terra will be performed, including the mapping of multi-ring impact basins. Other CRISM clay signature clusters, in Nili Fossae and Tyrrhena Terra, will be investigated. Besides CRISM clay signatures also other past hydrothermal activity 'signals' in impact craters will be used.

Acknowledgements: We are very grateful to Bethany L. Ehlmann providing the data points from [7].

References: [1] Schulze-Makuch D. et al. (2007) *Icarus 189, 308–324.* [2] Solomon S.C. et al. (2005) *Science 307, 1214–1220.* [3] Robbins S.J. and Hynek, B.M. (2012) *JGR 117*. [4] Rossi A.P. et al. (2008) *JGR, 113, E08016*. [5] Di Achille G. and Hynek, B.M. (2010) *Nature Geosci. 3, 459–463*. [6] Cabrol N.A. and Grin E.A. (1999) *Icarus 142, 160–172*. [7] Ehlmann B.L. et al. (2012) *Space Sci. Rev. 174, 329-364*. [8] Farmer J.D. (1996) *in: Ciba Foundation Symp. 202, 273–303*. [9] Carranza E.J.M. (2009) *Ore Geol. Rev. 35, 383–400*. [10] Debba P. et al. (2008) *Math. Geosci. 41, 421–446.* [11] Burkardt J. (2010) *http://people.sc.fsu.edu/~jburkardt/m_src/sphere_grid/sphere_grid.html* [12] Kuskov A. et al. (2005) *http://www.kuskov.com/content/view/61/65/* [13] R Core Team (2012) *http://www.R-project.org*. [14] de Souza Filho C.R. et al. (2012) *http://www.ige.unicamp.br/sdm/default_e.htm.* [15] Jenness, J (2012) *www.jennessent.com/arcgis/arcgis_extensions.htm.* [16] Knapmeyer M. et al. (2006) *JGR 111*.